

REACTION ENHANCED VAPORIZATION OF MOLTEN SALT

J.H. CAMERON

*The Institute of Paper Chemistry
Appleton, Wisconsin 54912*

(Received August 17, 1986; in final form May 1, 1987)

Vaporization of molten salts results in serious problems in the operation of many combustion systems. Salt vaporization of special importance in the burning of kraft black liquor, where combustion occurs in a molten $\text{Na}_2\text{S}/\text{Na}_2\text{CO}_3$ environment.

In this paper, it is shown that the vaporization of alkali carbonate during air oxidation of $\text{Na}_2\text{S}/\text{Na}_2\text{CO}_3$ results from Na oxidation in the gas phase. Oxidation of Na in the gas phase significantly lowers the partial pressure of Na. Since the driving force for vaporization is the difference between the equilibrium vapor pressure of Na at the gas-melt interface and the partial pressure of Na in the gas phase, this reduction in partial pressure of Na significantly increases Na vaporization rates and allows fuming to proceed with only mild reducing conditions in the melt.

KEYWORDS Inorganic Molten Salts Vaporization Fume

INTRODUCTION

Salt vaporization is an important phenomenon in many combustion processes. One of the combustion processes where salt vaporization is especially critical is the burning of kraft black. In the recovery process, the black liquor from the pulping process is burned in a recovery furnace. In the furnace, the combustion of the carbonaceous char produced from the pyrolysis of the black liquor occurs in a molten salt environment consisting principally of Na_2CO_3 and Na_2S . During the burning of the kraft black liquor a large quantity of fume particles are produced from the volatilization and condensation of the inorganic sodium compounds. These particles are typically 0.25 to $1.0\ \mu\text{m}$ in diameter and are composed principally of Na_2CO_3 and Na_2SO_4 .

Fume significantly affects the design and operation of the recovery furnace. These particles form deposits on the heat transfer surfaces, reducing heat transfer rates and increasing the amount of surface area required for a given steam load. The fume particles that do not deposit on the heat transfer surfaces are collected by the electrostatic precipitators and recycled into the black liquor. This increases the inorganic content of the black liquor and reduces its heating value on a unit weight basis.

Not all aspects of fume are detrimental. The beneficial aspect of the fume is that it captures the sulfur gases released during black liquor pyrolysis and combustion. This occurs through the reaction of Na_2CO_3 with SO_2 and O_2 to form Na_2SO_4 . This Na_2SO_4 is then removed by the precipitators and recycled back into the black liquor.

Recent work by Clay *et al.* (1984) and Cameron *et al.* (1985) has shown that air oxidation of Na_2S in a $\text{Na}_2\text{S}/\text{Na}_2\text{CO}_3$ melt can produce large quantities of Na_2CO_3 considerably greater than the rate under strongly reducing conditions. This phenomenon was unexpected and very difficult to interpret in terms of the existing concept of fume formation by elemental Na formation and volatilization at high-temperature reducing conditions. This paper describes the mechanism responsible for fume generation during air oxidation of Na_2S in a $\text{Na}_2\text{S}/\text{Na}_2\text{CO}_3$ melt.

PREVIOUS WORK

Several researchers have used thermodynamic equilibrium calculations to predict the liquid and gaseous species present in the kraft furnace. Bauer and Dorland (1964) were one of the first to apply this technique to the kraft furnace. Their study predicted that the volatile fuming species in the furnace are Na and Na_2 . They considered NaOH as a liquid species but not as a gaseous species. Thus they a priori eliminated it as a potential source of fume.

More recently Warnqvist (1973) also applied equilibrium thermodynamics to the kraft furnace and concluded that in addition to Na and Na_2 , NaOH is an important volatile compound. Warnqvist believed that the earlier study by Bauer and Dorland (1964) was flawed for not including NaOH(g) in the equilibrium calculations.

As stated by Warnqvist (1973) a major assumption in these equilibrium treatments is that "the waste liquor/air (oxygen) system as a whole comes to chemical equilibrium." This assumption is recognized to be somewhat unrealistic, but Warnqvist believed that this technique provides an insight into the processes and chemical species present in the furnace.

Equilibrium treatments predict that the major fume producing species are Na, Na_2 , and NaOH. The vaporization rate of a chemical species can be significantly affected by the reaction between the volatile species and any gaseous species, as indicated by Turkdogan (1963). Turkdogan (1980) states that there are two possible mechanisms for enhanced vaporization of a liquid into a reactive gas: (1) the gas may react with the liquid to form a volatile species or (2) the gas may react with the vapor from the liquid, lowering the partial pressure of the vapor above the liquid and enhancing the vaporization rate.

Turkdogan *et al.* (1963, 1980, 1982) have shown that the oxidation of many molten metals can produce large amounts of metal oxide fume. Since there are several similarities between these fuming systems and fuming during sulfide oxidation in a carbonate melt, a review of fuming during oxidation of molten metals is included here.

The increase in fuming during oxidation of molten metals is attributed to the reaction of the metal vapor with oxygen to form a condensed metal oxide fume. This may be considered to be a counterflux transport process. Oxygen diffuses toward the molten metal surface, and metal vapor diffuses away from the surface.

At some distance from the surface the metal vapor and O_2 react to form a metal oxide condensed phase. This reaction in the gas phase forms a sink for the metal vapor, reducing its partial pressure. Since the driving force for vaporization is the difference between the vapor pressure of the metal and its partial pressure in the gas phase, this reduction in partial pressure can greatly enhance the rate of vaporization.

The maximum rate of the metal vaporization with this mechanism is equal to the vaporization rate in a vacuum. At the maximum vaporization rate, the metal oxide fume is formed in the gas phase at the gas-metal interface. If the O_2 partial pressure is increased beyond this value, the flux of O_2 toward the metal surface is greater than the vaporization rate of the metal. Oxidation then occurs within the molten metal, forming a metal oxide film. Since the concentration of the volatile species is greatly reduced in this metal oxide film, the formation of this film results in a significant decrease in the vaporization rate of the metal.

EXPERIMENTAL APPARATUS

The fume generation experiments were conducted by monitoring the fume produced from alkali carbonate/sulfate/sulfide melts under different atmospheres. The experimental system consisting of an induction heated reactor, gas meters and fume filter is illustrated in Figure 1.

Two configurations for introducing the purge into the reactor were employed during this study. These configurations consisted of either introducing the N_2/O_2 gas mixture directly into the melt or into the reactor above the melt. Figure 1 illustrates the experimental system with the gases introduced below the melt's surface. With the gases introduced below the melt's surface, the O_2 in the purge was totally consumed by sulfide oxidation. With the gases introduced above the melt, the sulfide content of the melt was oxidized without any significant mixing of the melt.

The fume generation rate was followed by filtering the off-gas and weighing the fume particles. To ensure that this gravimetric method collected all the fume

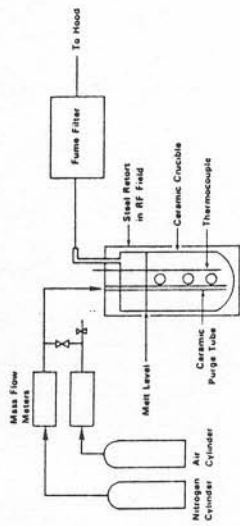


FIGURE 1 Experimental system.

REACTION ENHANCED VAPORIZATION

J.H. CAMERON

246

particles, the Na content of the off-gas after the filter was checked with a flame photometer. Readings from the flame photometer showed that the filter collected essentially all the fume particles.

The fume particles collected during sulfide oxidation were typically white spherical particles approximately 0.25 to 1.0 μm in diameter. Infrared analysis of the fume particles revealed that they are essentially pure Na_2CO_3 .

FUME GENERATION WITH GAS INTRODUCED BELOW THE MELT'S SURFACE

In this section, the effects of sulfide concentration, sulfate concentration, temperature, inlet oxygen content, and gas flow rate on fume generation with the gas introduced directly into the melt are described.

Typical Experimental Results with Gas Introduced Below the Melt's Surface

In a typical experiment, the fume generation rate was monitored by filtering the off-gas from the reactor for a five-minute period and weighing the fume collected. Experimental results typical of the majority of the experiments conducted using this procedure are illustrated in Table I.

It can be seen that the fume generation rate remains at a constant level until the sulfide is nearly totally oxidized. Once the sulfide level reaches a concentration of approximately 0.1 mole/L, the fume generation rate rapidly decreases. Although the relative concentrations of sulfide and sulfate change significantly during this experiment, little change in the fume generation rate is observed until the sulfide is nearly completely oxidized. This indicates that the ratio of sulfide to sulfate has little effect on the fume generation rate.

TABLE I

Typical experimental fume generation results with purge introduced below the melt's surface

Time, s	Calculated composition		Fume generation rate, g/min	Fume concentration Moles Na_2CO_3	
	Na_2SO_4 , mole/L	Na_2S , mole/L		Mole Na_2S	Mole Na_2CO_3
755	0.136	0.549	0.0099	0.00214	0.00011
1280	0.231	0.455	0.0104	0.00224	0.00011
1760	0.318	0.368	0.0106	0.00288	0.00011
2240	0.405	0.281	0.0104	0.00224	0.00011
2721	0.492	0.195	0.0099	0.00214	0.00011
3114	0.563	0.124	0.0088	0.00190	0.00011
3639	0.656	0.029	0.0005	0.00011	0.00011

Run 38
Initial Melt Composition
 $\text{Na}_2\text{CO}_3 = 0.77$ mole
 $\text{Na}_2\text{S} = 0.03$ mole
Purge = 1 L/min at 2.1% O_2
Temperature = 927°C

TABLE II

Effect of oxygen level in the purge on fume generation rate

Run	Temperature = 927°C		Fume generation rate, g/min
	N_2 , L/min	O_2 , L/min	
45	1.02	0.0105	0.00892
46	1.02	0.021	0.0105
47	1.02	0.042	0.0121
48	1.01	0.063	0.0145
49	1.02	0.084	0.0146

Effect of Oxygen Partial Pressure on Fume Generation Rate

To determine the effect of inlet O_2 concentration on the rate of fume generation, the O_2 level in the purge was varied. Preliminary studies of sulfide oxidation with O_2/N_2 mixtures introduced below the melt's surface have shown that essentially all the O_2 supplied to the melt is consumed by sulfide oxidation. Therefore, to maintain a constant off-gas flow rate from the melt, the N_2 flow to the reactor was held constant and the O_2 flow was adjusted. The results of a series of experiments with varying inlet O_2 concentrations are shown in Table II.

As shown in this table, the increase in O_2 to the reactor tends to increase the rate of fume generation. However, the fume dependence on the O_2 concentration rate is slight.

Effect of Nitrogen Flow Rate on Fume Generation

To determine the effect of the volumetric flow rate on the fume generation rate, the N_2 flow rate was varied while the O_2 flow rate was held constant. Since the oxidation rate is fixed by the amount of O_2 supplied, the oxidation rate remained the same for each experiment. The results of these experiments are given in Table III.

TABLE III

Effect of N_2 purge rate on fume generation.

Initial melt conditions: $\text{Na}_2\text{CO}_3 = 0.77$ mole
 $\text{Na}_2\text{S} = 0.03$ mole
Temperature = 927°C

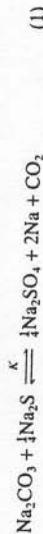
Run	N_2 , L/min	Air, L/min	Total N_2 , L/min	Fume generation rate \pm Std. Dev., g/min	
				Rate	Std. Dev.
50	0.04	0.1	0.48	0.00680 \pm 0.00032	0.00076
51	0.6	0.1	0.68	0.00850 \pm 0.00042	0.00076
52	0.8	0.1	0.88	0.01004 \pm 0.00042	0.00076
53	0.9	0.1	0.98	0.01024 \pm 0.00032	0.00042
54	1.06	0.1	1.14	0.01204 \pm 0.00042	0.00042
54	1.23	0.1	1.31	0.01474 \pm 0.00198	0.00198

The enhancement of fume generation observed during sulfide oxidation results from the oxidation of Na in the gas phase. This oxidation greatly lowers the partial pressure of Na in the gas phase, increasing Na vaporization from the melt.

Sodium sulfide in the melt is a sufficiently strong reducing agent to produce a significant Na partial pressure. The liquid and gas phase processes occurring during oxidation-enhanced fume generation are illustrated in Figure 3. Sodium and CO_2 are generated in the melt from the equilibrium reaction between Na_2CO_3 and Na_2S . The Na and CO_2 then evaporate and react with O_2 diffusing toward the melt. A detailed description of this fume generation mechanism is presented below.

Liquid Phase Processes

The processes responsible for fume generation during sulfide oxidation can be separated into those processes occurring in the liquid phase and those occurring in the gas phase. In the liquid phase, the concentration of Na in the melt is assumed to be dependent on the equilibrium given by Eq. (1).



Since the melt used for this study consisted primarily of Na_2CO_3 , the activity of Na_2CO_3 is assumed to be approximately 1.0. Then assuming ideal behavior for the Na_2S and Na_2SO_4 , the partial pressure for sodium is described by Eq. (2).

$$P_{\text{Na}} = \frac{K^{1/2} [X_{\text{Na}_2\text{S}}]^{1/2}}{[X_{\text{Na}_2\text{SO}_4}]^{1/2} [P_{\text{CO}_2}]^{1/2}} \quad (2)$$

Here, P_M is the partial pressure of component M ; X_M is the mole fraction of component M ; and K is a constant.

Gas Phase Processes

The most significant process occurring in the gas phase is the oxidation of Na, which lowers the partial pressure of Na in the gas. Since the rate of Na

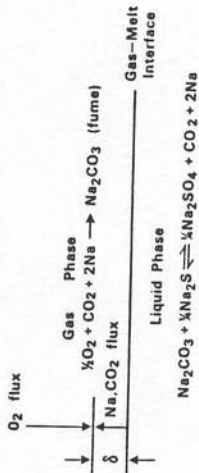


FIGURE 3 Fume generation under oxidizing conditions.

vaporization depends on the difference between the vapor pressure of Na at the melt-gas interface and the partial pressure in the gas, the reduction in partial pressure increases the Na vaporization rate.

The reactions occurring in the gas phase are represented by Eq. (3) and Eq. (4).



These equations are not intended to represent a mechanism, but are intended to indicate the stoichiometry of the gas phase reactions.

APPLICATION OF FUME GENERATION THEORY TO THE EXPERIMENTAL RESULTS

Interpretation of Fume Generation with Gas Introduced above Melt's Surface

The fume generation behavior observed with the gas introduced above the melt is very similar to that reported in Turkdogan's (1963) study of fuming during the oxidation of molten metals. At low O_2 partial pressure, the Na evolving from the melt is oxidized above the melt, lowering the partial pressure of Na and increasing the rate of Na vaporization. At higher O_2 partial pressures, the O_2 penetrates to the melt surface. Oxidation of the Na and Na_2S then occurs in the melt and little fume is generated.

Interpretation of Fume Generation with Gas Introduced below Melt's Surface

The fuming behavior during sulfide oxidation with the gas introduced below the melt's surface was considerably different than that observed with the gas introduced above the melt. The major difference was the relatively high level of fuming during Na_2S oxidation. The effect of O_2 partial pressure was also significantly different in the two modes of gas-melt contact. With the gas stream introduced below the melt's surface, increasing the O_2 partial pressure in the purge resulted in a slight increase in the rate of fume generation. This contrasts to the decrease in fume generation with an increase in O_2 partial pressure when the gas was introduced above the melt. The Na_2S concentration in the melt had different effects on the rate of fuming in the two modes of melt-gas contact. With the gas introduced above the melt, fuming rate decreased as the Na_2S was oxidized to Na_2SO_4 . With the gas introduced below the melt's surface, the level of Na_2S concentration had no effect on the fuming rate until only low levels of Na_2S remained in the melt.

With the gas introduced below the melt's surface, fume is generated in the bubble as it rises in the melt. The liquid surrounding the bubble is continually renewed, and as a result of the liquid flowing past the bubble the gas in the bubble may undergo toroidal circulation. The basic difference between this mode

TABLE IV
Effect of two purge tubes on fume generation rate

Run no.	Temp., °C	N ₂ flow rate, L/min	O ₂ flow rate, L/min	Fuming rate, g/min ± Std. Dev.	Fuming rate with single purge tube, g/min
127	953	1.03	0.020	0.0129 ± 0.001	0.0126
128	957	1.03	0.0426	0.0163 ± 0.001	0.0156
129	957	1.01	0.0634	0.0156 ± 0.001	0.0172

It is evident that the fume generation rate is nearly proportional to the volumetric purge rate.

Surface Area Effect

The objective of these experiments was to determine if a change in the surface area of the bubbles would affect the fume generation rate. To increase the melt-gas interface, the single purge tube (0.476-cm ID) was replaced with two purge tubes (0.158-cm ID).

The fume generation rates from several sulfide oxidation experiments employing the two purge tubes are shown in Table IV. Also shown in this table are the fume generation rates for the single purge tube.

It can be seen that the fume generation rate using the two purge tube system is nearly the same as that for the single purge tube. Therefore, changes in the melt-gas interfacial area have little effect on the fume generation rate.

FUMING WITH OXYGEN-NITROGEN GAS INTRODUCED ABOVE MELT'S SURFACE

To determine the effect of the mode of gas-liquid contact on oxidative fuming, fume generation during sulfide oxidation was studied with the purge tube located above the melt. Typical fume generation rates during sulfide oxidation using this mode of gas-melt contact are illustrated in Figure 2.

This figure shows that the oxidation of a sulfide in a sulfide-carbonate melt with the O₂ introduced above the melt usually results in a decrease in the fume generation rates compared to that observed under a pure N₂ purge. Only at extremely low levels of O₂ did the fume generation rate increase. This is in distinct contrast to the large level of fume observed when the gas was introduced into the melt.

With the purge located above the melt's surface, approximately half of the O₂ in the purge was consumed through sulfide oxidation. By varying the O₂ content of the purge, fume generation rates with the purge located above the melt were compared at the same oxidation rate to those generated with the purge located below the melt's surface. It was found that the fume generation rates with the

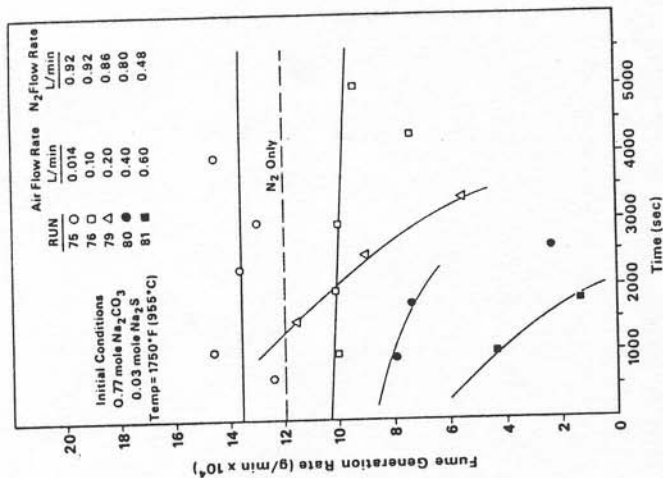


FIGURE 2 Effect of oxygen on fume generation with purge introduced above melt.

purge introduced above the melt's surface are approximately an order of magnitude lower than those with the purge introduced below the melt's surface.

Equal rates of sulfide oxidation can be achieved with both modes of gas-melt contact. Therefore, if fume results from the formation of a volatile species during sulfide oxidation, this species should be formed in both modes of gas-melt contact. Since little fume is generated when the gas is introduced above the melt's surface, it is unlikely that fume generation during sulfide oxidation results from the formation of a new volatile compound.

MECHANISM FOR FUME GENERATION UNDER OXIDIZING CONDITIONS

Based on the experimental results obtained in this study, the following theory is proposed to explain fume generation during sulfide oxidation:

of oxidation and oxidation with the gas introduced above the melt is the mixing of the liquid at the gas-melt interface.

With purge tube located below the melt, Na evolves from the melt and is oxidized near the interface in the gas. This oxidation lowers the partial pressure of Na in the gas and significantly enhances the rate of Na evolution. Since the melt at the interface is constantly renewed, its composition remains constant as the O₂ in the bubble is consumed. The fume generation rate is constant as long as sufficient O₂ remains in the gas to rapidly oxidize the Na evolving from the melt. The fume generation rate observed then depends on the time required for consumption of the O₂ in the bubble.

The rate of O₂ consumption is described by Eq. (5).

$$\frac{d(N_{O_2})}{dt} = SKg(P_{O_2} - P_{O_2}^*) \quad (5)$$

Here, P_{O_2} is the partial pressure of O₂ in the bulk gas; $P_{O_2}^*$ is the partial pressure at the interface; Kg is the gas phase mass transfer coefficient; N_{O_2} is moles of O₂; and S is interfacial surface area.

Since $P_{O_2} \gg P_{O_2}^*$, Eq. (6) can be written as:

$$\frac{d(N_{O_2})}{dt} = SKgP_{O_2} \quad (6)$$

The partial pressure of O₂ in the gas is shown in Eq. (7):

$$P_{O_2} = \frac{N_{O_2}}{N_{N_2} + N_{O_2}} \times Pt \quad (7)$$

Here, Pt is the total pressure, and N_{N_2} is moles of N₂.

For the experimental conditions used in this study the O₂ content in the gas during sulfide oxidation is much less than the N₂ content of the gas. The partial pressure of O₂ is then approximated by Eq. (8).

$$P_{O_2} = \frac{N_{O_2}}{N_{N_2}} Pt \quad (8)$$

The rate of O₂ consumption is then given by Eq. (9)

$$\frac{d(N_{O_2})}{dt} = SPtKg \frac{N_{O_2}}{N_{N_2}} \quad (9)$$

During sulfide oxidation, the fume generation rate remains constant until the O₂ level in the gas bubble falls below that required to rapidly oxidize the Na being evolved. The weight loss of the melt due to fuming (or fume generated during this period) is then described by Eq. (10).

$$\frac{dF}{dt} = -SK \quad (10)$$

Here, F is the weight of material evolved from the melt during the fuming period, and K is a constant.

Dividing Eq. (10) by Eq. (9) gives the change in fume with the O₂ content of the gas bubble, Eq. (11)

$$\frac{dF}{d(N_{O_2})} = -\frac{KN_{N_2}}{KgPtN_{O_2}} \quad (11)$$

Once the O₂ level in the bubble falls to the level where the Na evolved is not oxidized, fume generation essentially stops. Equation (11) can then be integrated between the following boundary conditions.

1. For initial moles of O₂ in bubble ($N_{O_2,i}$), fume generation (F) = 0. This boundary condition is simply that no fume is generated until the gas is introduced into the melt and the oxidation process begins.

2. For O₂ remaining in bubble when fuming stops ($N_{O_2,r}$), fume generated = measured fume (F_M). This condition is that once the O₂ concentration in the bubble falls below that required to rapidly oxidize the Na evolving from melt, fuming stops and the fume present in the bubble is the measured fume F_M .

$$\int_{N_{O_2,r}}^{N_{O_2,i}} dF = -\frac{KN_{N_2}}{kgPt} \int_{N_{O_2,r}}^{N_{O_2,i}} \frac{dN_{O_2}}{N_{O_2}} \quad (12)$$

$$F_M = \frac{KN_{N_2}}{KgPt} [\ln(N_{O_2,i}) - \ln(N_{O_2,r})] \quad (13)$$

To test this model of fume generation, the fume generation rates were plotted vs. the ln of the initial O₂ flow rates, Figure 4, for three different carrier gases. From Eq. (13), this plot of the ln of the initial O₂ molar flow rates vs. the fume generation rate should yield a straight line.

As illustrated in Figure 4, Eq. (13) accurately describes the effect of O₂ on fume generation during sulfide oxidation with the purge introduced below the melt's surface. In Figure 4, fume generation is clearly a logarithmic function of the initial O₂ content of the purge.

The lower fume generation rate in He is due to O₂ having a higher diffusivity in He than it has in either Ar or N₂. This higher diffusivity results in faster consumption of the O₂ and hence a shorter time for fume generation.

The penetration theory first proposed by Higbie (1935) predicts that the mass transfer coefficient should be proportional to the square root of the diffusivity, as given by Eq. (14).

$$K_s \propto D^{1/2} \quad (14)$$

Then from Eq. (13), the fume generated as the bubble passes through the melt should be inversely proportional to the square root of the interdiffusivity of O₂ in the carrier gas.

To confirm this, the diffusivities for O₂ in the three inert carrier gases were calculated using the Wilke and Lee (1955) modification of the equation by Hirschfelder, Bird and Spontz (1949).

Table V lists the calculated diffusivities of O₂ in the three carrier gases used in this study, the predicted fuming rates relative to the N₂-O₂ system, and the actual fuming rates relative to the N₂-O₂ system. The actual relative fuming rates in this

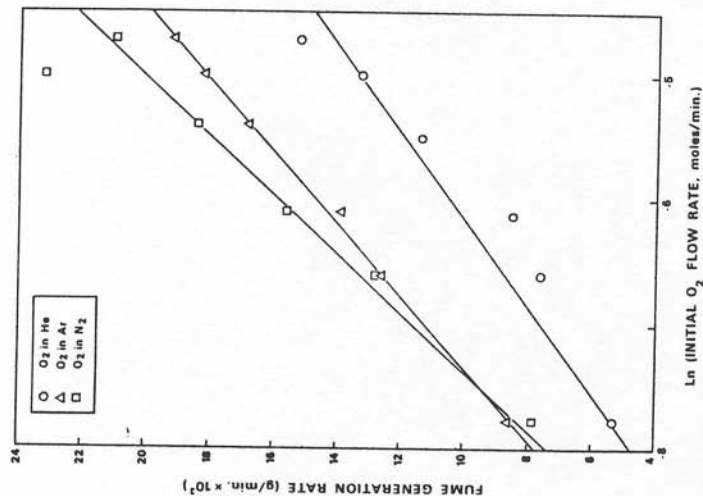


FIGURE 4 Effect of O_2 on fume generation in N_2 , Ar, and He.

table are the averages of the relative fuming rates for different O_2 levels. The predicted relative fuming rates are based on the change in the gas mass transfer coefficient resulting from changes in the diffusivities of O_2 in the carrier gases. As shown in this table, the actual relative fuming rates are quite close to those predicted on the basis of changes in O_2 diffusivities in the carrier gases.

DISCUSSION

This mechanism for enhanced fuming under oxidizing conditions accurately explains the effects of the experimental variables on fume generation during sulfide oxidation. The major effects of the experimental variables on fume generation and their relationship to the proposed mechanism are summarized below.

(A) Fume generation during sulfide oxidation with the N_2 - O_2 gas system introduced above melt's surface.

1. Fume generation with a N_2 - O_2 gas was normally less than that with a pure N_2 . This results from the sulfide oxidation rate being liquid side mass transfer limited in this mode of gas-melt contact. The melt at the gas-melt interface is oxidized and the vapor pressure of Na is low in this oxidized state.
2. Only at very low O_2 partial pressures was the fume generation rate greater than that with a N_2 atmosphere. This results when the low O_2 partial pressures are not sufficient to oxidize the melt's surface. Sodium then vaporizes from the melt and is oxidized in the gas above the melt. This creates a Na sink and increases the rate of Na vaporization.

(B) Fume generation during sulfide oxidation with the N_2 - O_2 gas introduced below the melt's surface.

1. Sulfide oxidation in this mode of gas-melt contact produces large quantities of fume. This results from sulfide oxidation being gas-side mass transfer limited. The melt at the gas-melt interface has a relatively high Na vapor pressure. As soon as this Na evolves from the melt it is oxidized in the gas phase. This oxidation drastically lowers the partial pressure of the Na in the gas and increases the vaporization rate.
2. The rate of fuming is nearly proportional to the N_2 purge rate. This results from the rate of oxygen consumption in the gas bubble being inversely proportional to the N_2 flow rate, Eq. (9). Therefore, as the N_2 purge rate increases, the time required for complete consumption of the O_2 in the gas is also increased and more fume is generated.
3. The fume generation rate depends logarithmically on the initial O_2 content of the gas. This results from the rate of consumption of O_2 in the gas bubble being proportional to the O_2 concentration. The rate of O_2 consumption is then a logarithmic function. This logarithmic dependence of the fuming rate is predicted by Eq. (13).
4. The bubble size and hence surface area had no effect on the fume generation

TABLE V
Effect of gas diffusivity of fume generation

Gas system	Diffusivity \pm av. error, cm^2/s	Predicted relative to N_2 - O_2 fuming rates, g/min	Actual relative to N_2 - O_2 fuming rates, ± 1 Std. Dev., g/min
N_2 - O_2	2.44 ± 0.1	1.0	1.0
Ar- O_2	2.38 ± 0.1	1.01	0.93 ± 0.10
He- O_2	8.08 ± 0.3	0.55	0.58 ± 0.07

rate. This results from the rate of sulfide oxidation, Eq. (9), and the rate of fume generation, Eq. (10), both being directly proportional to the surface area. Since the surface area drops out when these equations are combined, Eq. (11), the surface area of the gas bubble does not affect the fume generation rate.

5. Fume generation during sulfide oxidation is not highly dependent on the Na_2SO_4 and Na_2S content of the melt. This results from the very weak dependence of Na vapor pressure on the concentration of these compounds, Eq. (2).

6. Carrier gases with higher O_2 interdiffusivities produce lower fume generation rates. This results from higher interdiffusivities producing faster rates of O_2 consumption. Since the O_2 in the bubble is consumed faster, fuming lasts for a shorter period of time and less fume is produced.

The experimental results of this study demonstrate that enhanced fume generation during Na_2S oxidation results from the Na oxidation in the gas phase. Although fume generation was studied in rising gas bubbles, the mechanism for enhanced fume generation can occur anytime an oxidizing atmosphere contacts a reduced melt. All this mechanism requires is that there is enough mixing in the melt that the melt's surface is renewed faster than it is oxidized. This may occur anytime turbulent conditions exist. Therefore, this mechanism likely has a significant effect on the amount of fume generated in the kraft furnace. Since furnace gases such as O_2 and CO_2 are reactive with Na and Na_2S , equilibrium treatments cannot be used to predict the amount of fume generated through Na and Na_2 vaporization. They can, however, be used to predict the melt composition and the vaporization rate of nonreactive species such as KCl, NaCl, and possibly NaOH.

NOMENCLATURE

D_A	Diffusivity
F	Fume evolved
F_M	Measured fume
K	Constant
K_A	Mass transfer coefficient
K_g	Mass transfer coefficient, Eq. (5)
N_{N_2}	Moles of N_2
N_{O_2}	Moles of O_2
N_{O_2f}	Moles of O_2 in bubble when fuming stops
N_{O_2i}	Initial moles of O_2 in bubble
P_{O_2}	Partial pressure of O_2
$P_{O_2}^*$	Partial pressure of O_2 at the interface
P_t	Total pressure

S	Surface area
t	time
X_M	Mole fraction of component M

REFERENCES

- Bauer, T.W., and Dorfand, R.M., *Can. J. Techn.* **32**, 91 (1954).
- Cameron, J.H., Clay, D.T., and Grace, T.M., 1985 International Chemical Recovery Conference 11-2, 435; New Orleans, LA.
- Clay, D.T., Grace, T.M., and Kapheim, R.J., *AIChE Symposium Series* **239**, 80, 99 (1984).
- Hirschfelder, J.O., Bird, R.B., and Spotz, E.L., *Trans. Am. Soc. Mech. Engrs.* **71**, 921 (1949).
- Turkdogan, E.T., Grieveson, P., and Darken, L.S., *J. Phys. Chem.* **67**, 1647 (1963).
- Turkdogan, E.T., *Physical chemistry of high temperature technology*, Academic Press, New York, 1980.
- Turkdogan, E.T., Grieveson, P., Darken, L.S., *Proc. Natl. Hearst Steel Con.* **470** (1982).
- Warnqvist, B., *Svensk Papperstid.* **76**(12), 463-6 (1973).
- Wilke, C.R., and Lee, C.Y., *Ind. Eng. Chem.* **47**, 1253 (1955).